OFFSHORE RADIATION OBSERVATIONS FOR CLIMATE RESEARCH AT THE CERES OCEAN VALIDATION EXPERIMENT

A New "Laboratory" for Retrieval Algorithm Testing

BY CHARLES K. RUTLEDGE, GREGORY L. SCHUSTER, THOMAS P. CHARLOCK, FREDERICK M. DENN, WILLIAM L. SMITH JR., BRYAN E. FABBRI, JAMES J. MADIGAN JR., AND ROBERT J. KNAPP

NASA's Clouds and the Earth's Radiant Energy System program is performing high-quality surface radiation monitoring in support of climate change research on an ocean platform off of Virginia's coast.

The National Aeronautics and Space Administration's (NASA's) Clouds and the Earth's Radiant Energy System (CERES) project is observing the radiant energy leaving the Earth's atmosphere. CERES produces an archive of the radiation budget, from the bottom to the top of the atmosphere, with high temporal and spatial resolution for multiple years, with an accuracy necessary for climate change research (Wielicki et al. 1996). One expected payoff from analyzing this archive will be a new level of understanding of how clouds and aerosols affect the planet's energy budget. Climate theory indicates that the veracity of a climate model hinges strongly on the accuracy of the radiation budget simulated by the model. CERES data are a key test bed for such models. To fill the test bed with quality data, much is required.

The parameters needed to fill the CERES archive, such as irradiances at various altitudes within the atmosphere's column, are not directly measured by the CERES instruments that are presently circling the planet on several of NASA's Earth Observing System (EOS) satellites [Tropical Rainfall Measuring Mission (TRMM), *Terra,* and *Aqua*]. "Retrieval algorithms" that use the CERES measurements, ancillary data, and radiative transfer theory are required for this processing. These algorithms deal

AFFILIATIONS: RUTLEDGE, DENN, FABBRI, AND MADIGAN—Analytical Services and Materials, Inc., Hampton, Virginia; SCHUSTER, CHARLOCK, AND SMITH—NASA Langley Research Center, Climate Sciences Branch, Hampton, Virginia; KNAPP—Science Applications International Corporation, Hampton, Virginia
CORRESPONDING AUTHOR: Ken Rutledge, Suite 300, One Enterprise Parkway, Hampton, VA 23666
E-mail: c.k.rutledge@larc.nasa.gov

with intricacies like geolocation, viewing geometry, surface properties, sun glint, and the cloud aerosol and gaseous constituents of the atmosphere, as well as the incomplete spatial and temporal sampling of the planet by the satellites.

Apart from the operation and calibration of the satellite instruments, developing and testing the retrieval algorithms is a large part of the CERES effort. It would be ideal to test the algorithms for retrieval processes in a sealed laboratory, where all of the relevant parameters could be easily measured. The size and complexity of the Earth make this impractical. CERES instead uses a few score sites worldwide, each with surface radiometers, as a virtual laboratory. One site is over the ocean.

An ocean site offers two characteristics that are important when trying to learn the most about the atmosphere from the vantage point of a satellite. In the visible and near-infrared wavelengths, constituents of the atmosphere alter the upwelling and downwelling radiation. From space, constituents (aerosols, clouds, water vapor, and molecular species) are easiest to detect over dark surfaces with uniform reflective properties. The ocean's surface meets these criteria, and land surfaces, which are brighter and more spatially inhomogeneous, generally do not.

The CERES Ocean Validation Experiment (COVE) is a new "laboratory" for long-term radiation observations in the ocean environment that benefits from the site's surface properties. COVE is implemented on the Chesapeake Lighthouse ocean platform located in the coastal Atlantic Ocean approximately 25 km off the Virginia coastline (Fig. 1). The small size of the ocean platform (tens of meters) offers another favorable characteristic for an ocean observation site compared to sites on small islands (thousands of meters). The ocean platform is so small that it does not affect its local weather as happens on many small islands. Because about 70% of the planet is covered by water, getting the remote sensing algorithms correct over the oceans is really important.

MODELS ARE KEY. The important energy quantities needed for atmospheric radiation budget research are the shortwave and longwave irradiances (see the appendix for the definition of terms). These quantify the radiant energy originating from the sun and from the Earth (plus constituents in the atmosphere). We need to know these irradiances at the top and surface of, and within, the atmosphere; they drive the general circulation and the hydrological cycle. Radiation can be absorbed or emitted, and it may change directions by scattering (off constituents in the atmosphere) or reflecting (off the surface). There are typically errors of 1% or more in our observations and models of vital irradiances.

The CERES instruments measure planet-leaving energy as radiances in the shortwave and longwave regions of the electromagnetic spectrum at the top of the atmosphere (TOA). As the EOS satellites with CERES instruments aboard them circle the planet, the radiances are sensed at multiple angles below the satellites. Angular distribution models are used to convert the radiances to irradiances. Radiative transfer models are used to estimate upwelling and
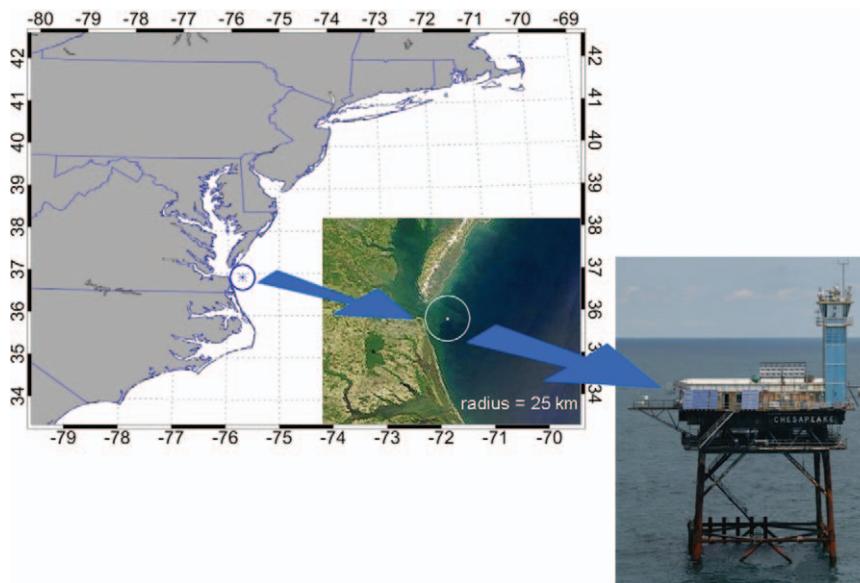
Fig. 1. The COVE site (36.905°N, 75.713°W) is located in the Atlantic coastal ocean due east of Virginia's border. The ocean platform serves as an aid-to-navigation facility marking an important southern entry shipping channel to the mouth of the Chesapeake Bay. Many of our instruments are located on the light room roof on the tower part of the ocean platform (blue structure on right side in the photo). A helicopter landing pad (approximately 27 m × 27 m) serves as a roof for the housing section of the lighthouse. Helicopters are used for transportation of personnel and small loads for safety reasons. We use boats only for transporting large loads of supplies or instruments. The ocean's depth close to the platform is only about 12 m.

downwelling irradiances at the planet's surface, at TOA, and within the atmosphere's column. Cloud retrieval models quantify the location, type, and properties of clouds in the atmosphere. COVE was established to test components of the retrieval processes within these models.

PLATFORM DESCRIPTION. The Chesapeake Lighthouse ocean platform is a rigid multilevel steel structure that was built in the mid-1960s by the U.S. Coast Guard as an important aids-to-navigation resource. Its large pylons sink about 70 m into the sandy ocean floor, and the highest point on the structure is about 37 m above the mean sea level. This height and stability are necessary so that the accurate pointing of instruments is possible (well above the breaking wave spray that sometimes occurs when the sea is rough). Ships and buoys simply cannot offer this stability. We have implemented self-contained power and communications systems to control instrumentation and access the data products obtained at the ocean platform.

OBSERVATIONS AT COVE. The quality of COVE data is enhanced by subscribing to the rigorous standards of several observation networks. Table 1

TABLE 1. List of current geophysical measurements at the Chesapeake Lighthouse (see appendix for definitions).

Measurement	Domain*	Instrument	Wavelengths (μm)	Network	COVE dataset
Passive radiation measurements					
Direct shortwave irradiance	A	Pyrheliometer	0.2–4	BSRN	Yes
Diffuse shortwave irradiance	A	Pyranometer	0.2–4	BSRN	Yes
Global shortwave irradiance	AO	Pyranometer	0.2–4	BSRN	Yes
Longwave irradiance	AO	Pyrgeometer	5–50	BSRN	Yes
PAR irradiance	AO		0.4–0.7		Yes
Global and diffuse narrowband irradiance	AO	UV MFRSR	0.300–0.368 (7 bands)		Yes
Global and diffuse narrowband irradiance	AO	MFRSR	0.415–0.936 (6 bands)		Yes
Narrowband radiance	AO	Spectrophotometer	0.355–1.025 (17 bands)		Yes
Direct and diffuse narrowband radiance	AO	Sunphotometer	0.340–1.020 (7 bands)	AERONET	No
Microwave radiometer	A	MWR	Multiple		Yes
Active radiation measurements					
Aerosol backscatter and extinction profiles	A	Lidar	0.523	MPLnet	No
Total column precipitable water vapor	A	GPS		GPS-MET	No
Aerosol in situ measurements					
Number density	A	Condensation nuclei Counter			Yes
Potential cloud nuclei	A	Cloud condensation nuclei counter			Yes
Aerosol absorption coefficient	A	Aethalometer	0.37, 0.47, 0.52, 0.59, 0.88, 0.95		Yes
Aerosol extinction coefficient	A	Nephelometer	0.53		Yes
Average aerosol diameter	A	Electrical aerosol detector			Yes

*A: atmosphere, O: ocean, AO: atmosphere and ocean. BSRN: AERONET, GPS MET: ground-based meteorology; NDBC, NOAA; observations with no network association are NASA Langley projects.

lists the networks that operate at the COVE site and also the particular instruments involved. Over five years of continuous basic radiation observations have been collected at the site (beginning in April 2000). Standard meteorological data have been collected since 1984 by the National Oceanic and Atmospheric Administration's (NOAA's) National Data Buoy Center (NBDC). Time histories from the other observation networks operating at the site are not as long because they were added later. The multiple networks allow us to measure both the inputs and outputs of some of the parameters associated with the retrieval models mentioned above. Measuring the inputs and outputs allows for the detailed testing of the components of the retrieval processes for the radiant energy moving within the atmosphere and ocean. At times, special instrumentation and aircraft platforms have played an important part in the observations made at the COVE site (see the "Intensive Operations Periods" sidebar).

Surface irradiances. The broadband radiation observations at COVE follow the Baseline Surface Network (BSRN; see information online at http://bsrn.ethz.ch) calibration and sampling protocols (Ohmura et al. 1998; McArthur 2005). For the downwelling surface irradiances, dual solar trackers are presently deployed.

Pyrheliometers mounted on the solar trackers that maintain pointing toward the sun are used to obtain the direct solar irradiances. The same solar trackers provide shading mechanisms for shortwave pyranometers (for the diffuse irradiance measurement). The direct and diffuse measurements are combined to obtain the global downwelling shortwave irradiances at the surface. Dome-shaded pyrgeometers measure the downwelling longwave irradiances. Figure 2(A) shows the location of the downwelling irradiance sensors on the tower of the ocean platform. Sensors for measuring the photosynthetically active radiation (PAR) irradiances are also located on the tower top. These instruments measure the radiation that arrives at the surface from the atmosphere. These observations have been compared to the retrieved quantities output by the radiative transfer models used by CERES (see "Science problems" section).

To quantify the radiation that leaves the surface, upwelling observations of longwave irradiance (using a pyrgeometer) and shortwave irradiance (using a pyranometer) are located on a "catwalk" structure, which extends 8 m from the platform structure [Fig. 2(B)]. The downwelling broadband data are archived at the BSRN archive (Web page noted above); the other irradiance data can be obtained

INTENSIVE OBSERVATION PERIODS

CHESAPEAKE LIGHTHOUSE AND AIRCRAFT MEASUREMENTS FOR SATELLITES (CLAMS).
The CLAMS field campaign was conducted in summer 2001 to validate aerosol and radiation products derived from the Moderate Resolution Imaging Spectrometer (MODIS), Multiangle Imaging Spectroradiometer (MISR), and CERES instrument data taken from the EOS *Terra* spacecraft (Smith Jr. et al. 2005). The synergy of a comprehensive field campaign with multispectral imagery (MODIS), a multiangle sensor (MISR), and broadband accuracy (CERES) on a single spacecraft provides unprecedented data for diagnosing particular aspects of aerosol radiative forcing (i.e., Jin et al. 2005; Levy et al. 2005; Remer et al. 2005; Ignatov et al. 2005), which is a critical uncertainty factor in decadal-scale climate change.

The aircraft deployment around COVE during CLAMS included the MODIS airborne simulator (Gatebe et al. 2005) and the Airborne MISR (AirMISR) (Kahn et al. 2005) on NASA's ER-2 Airborne Science aircraft at 20 km; an interferometer in the high-resolution thermal infrared on the experimental Proteus for sensing temperature, humidity, and aerosol effects (Smith Sr. et al. 2005); the Ames Airborne Sunphotometer (AATS-14) remotely sensed spectral aerosol optical depth (Redemann et al. 2005) and in situ measurements of aerosol physical (Magi et al. 2005) and chemical (Castanho et al. 2005) properties on a CV-580 at various

altitudes; broadband pyranometers on a low-level OV-10 (Smith Jr. et al. 2005); and a photopolarimeter on a Cessna (Chowdhary et al. 2005). The ocean surface is the most ubiquitous boundary condition for solar photons approaching the Earth–atmosphere system, and both the brief CLAMS campaign and the continuous COVE platform provide a rigorous test bed for the remote sensing of aerosols and fluxes with *Terra* over that boundary condition. CLAMS data can be obtained from the NASA Langley Atmospheric Sciences Data Center (online at http://eosweb.larc.nasa.gov).
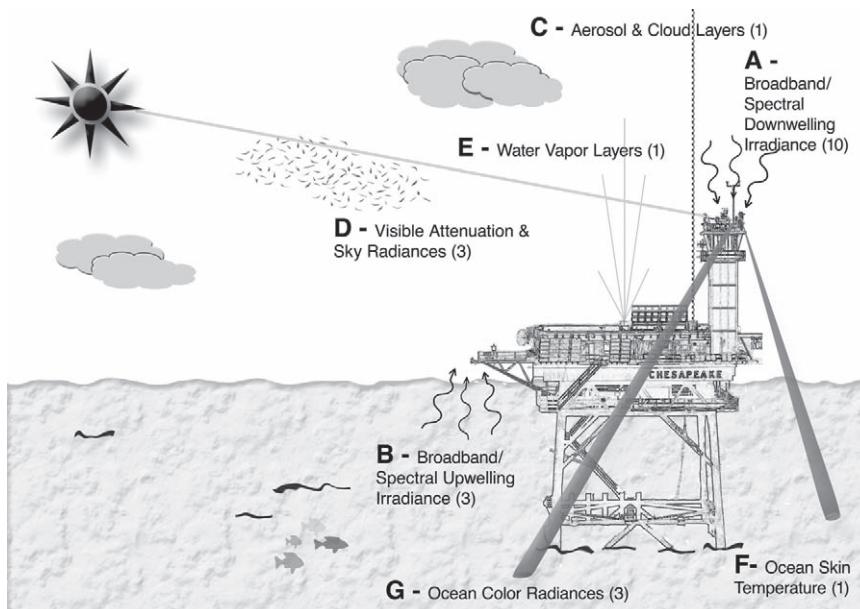
AIRS BALTIMORE BOMEM ATMOSPHERIC EMITTED RADIANCE INTEFEROMETER (BBAERI) OCEAN VALIDATION EXPERIMENT.
The AIRS BBAERI Ocean Validation Experiment (ABOVE) was conducted by the University of Maryland, Baltimore County during the summers of 2002 and 2003. In situ measurements were deployed at Chesapeake Lighthouse for validation of the AIRS instrument on the NASA EOS *Aqua* satellite. The instrument suite included the BBAERI, Elastic Lidar Facility, radiosondes, ozonesondes, carbon monoxide, and ozone gas samplers. In addition to *Aqua* validation, ABOVE measurements are being used for atmospheric pollution and transport process studies. Information on the ABOVE project can be found online at http://physics.umbc.edu/~mcmillan.

online at http://cove.larc.
nasa.gov. Measuring up-
welling and downwelling
shortwave spectral irradi-
ances with shadowband
radiometers resolves the
spectral distribution of
energy, which gives insight
on how well the models are
performing.

Aerosol and cloud layers.
NASA's Micropulse Lidar
Network (MPLnet) oper-
ates a lidar at the COVE site
for observations to learn
about the vertical structure
of clouds and aerosols in
the atmosphere. Measure-
ments of the backscatter-
ing of pulsed laser energy
determines the location of
aerosol and cloud particles
within the atmospheric
column at altitudes well
above those of standard
ceilometers (Welton et al.
2001). The instrument has
an unobscured vertically
pointing view from its po-
sition on the helicopter
landing pad near the tower
at COVE [Fig. 2(C)]. Profile
data are available online
at http://mplnet.gsfc.nasa.
gov/. These observations
provide inputs to the radia-
tive transfer models, which
need information about the
location of aerosols and clouds in the atmospheric
column above the COVE site.

FIG. 2. Locations of functional groups of sensors located at COVE (number of instruments per group): (A) instruments for observing downwelling irradi-ances view the entire sky hemisphere, some have optical domes or windows that are cleaned daily by an automated washing system, shortwave broad-band, longwave broadband, visible/UV spectral, and PAR; (B) instruments for observing upwelling irradiances view the entire ocean hemisphere, a problem exists because some of the "view" includes the legs of the platform and shadows from the platform contaminate the data before solar noon each day (these data are excluded from analyses), shortwave broadband, longwave broadband, visible spectral; (C) aerosol and cloud backscatter lidar, requires an environmentally controlled enclosure that maintains a set temperature to within ± 1° C (24 h day^{-1}, 365 days yr^{-1}) so that the optical components in its telescope do not expand or contract (and void the calibration); (D) optical extinction and radiance sunphotometers, a calibration site on Mauna Loa, HI, is used to cycle instruments through or an instrument calibrated at Mauna Loa is brought to the instruments (AERONET); (E) scanning microwave radiometer measures directional temperatures to produce altitude-depen-dent profiles of water vapor (using a model); (F) radiances of a portion of the longwave spectrum determine the skin temperature of the ocean's surface; (G) radiometers sense radiances at the ocean's surface to determine the water-leaving radiances at various narrowband wavelength intervals.

Visible attenuation and sky radiances. A Cimel sunpho-
tometer operating at the COVE site is part of NASA's
Aerosol Robotic Network (AERONET), a ground-
based network of radiometers located throughout the
world (Holben et al. 1998, 2001). The sunphotometer
is mounted on a programmable tracker enabling
direct sun measurements as well as sky radiance
measurements. This instrument system is located on
top of the tower at the COVE site [Fig. 2(D)]. Direct
sun measurements are used to retrieve multispectral
aerosol optical depths and total column precipitable

water when the path between the instrument and the
sun is free of clouds (Bruegge et al. 1992; Smirnov
et al. 2000). Sky radiance scans are input to retrieval
models to infer the fundamental optical properties
used to characterize the atmosphere [wavelength-
specific extinction optical thickness, single scattering
albedo, and the asymmetry factors (Dubovik and
King 2000; Dubovik et al. 2000)]. These optical char-
acteristics summarize the entire atmospheric column
above the COVE site. They may be partitioned into
atmospheric layers using the information retrieved
by the MPLnet lidar. This combined, layered optical
property information is a fundamental input required
for the radiative transfer models used by CERES. The

AERONET data archive available online at http://aeronet.gsfc.nasa.gov/ contains data from the COVE site since October 1999.

Water vapor and temperature (layers). Multiple sources of information for the water vapor content and atmospheric temperature structure are available at COVE. Radiosondes are launched during intensive operation periods (IOPs) to obtain profiles of temperature and relative humidity within the atmospheric column, but such IOPs are rare. We are unable to launch sondes from the site daily because it is unmanned. To find suitable profile information, we have compared COVE sonde temperature profiles to products provided by the *Goddard's Earth Observing System* (*GEOS*)-*4* (Bloom et al. 2005). Agreement within ± 1% was found for atmospheric pressures from 975 to 200 hPa (results not shown) for 27 temperature profiles observed during the month of July 2001. Without having actual sonde data, the *GEOS-4* data may be used to provide realistic column characterization for the COVE site.

NOAA's Global Systems Division Demonstration Branch (GSDDB) operates a global positioning system (GPS) receiver at the COVE site to determine the total column precipitable water vapor (Businger et al. 1996; Duan et al. 1996). The microwave signal suffers an atmospheric time delay in its transit from a satellite to the surface, and the magnitude of the delay is dependent upon the amount of water vapor. These data are available at the NOAA GSDDB GPS Meteorology Web site (online at www.gpsmet.noaa.gov/).

A scanning microwave radiometer [on short-term loan from the Department of Energy's Atmospheric Radiation Measurement (ARM) program] was recently deployed to retrieve profiles of water vapor and liquid water content [Fig. 2(E)]. These data are available on the COVE Web site. These profiles are necessary inputs to radiative transfer models when the optical properties of the atmosphere need to be inferred.

Ocean skin temperature. COVE operates an infrared radiation pyrometer for measuring sea surface temperature. The instrument is mounted on the tower top and points at the ocean's surface on the east side of the lighthouse [Fig. 2(F)]. The ocean skin temperature is used to verify surface longwave retrievals and longwave observations performed by CERES.
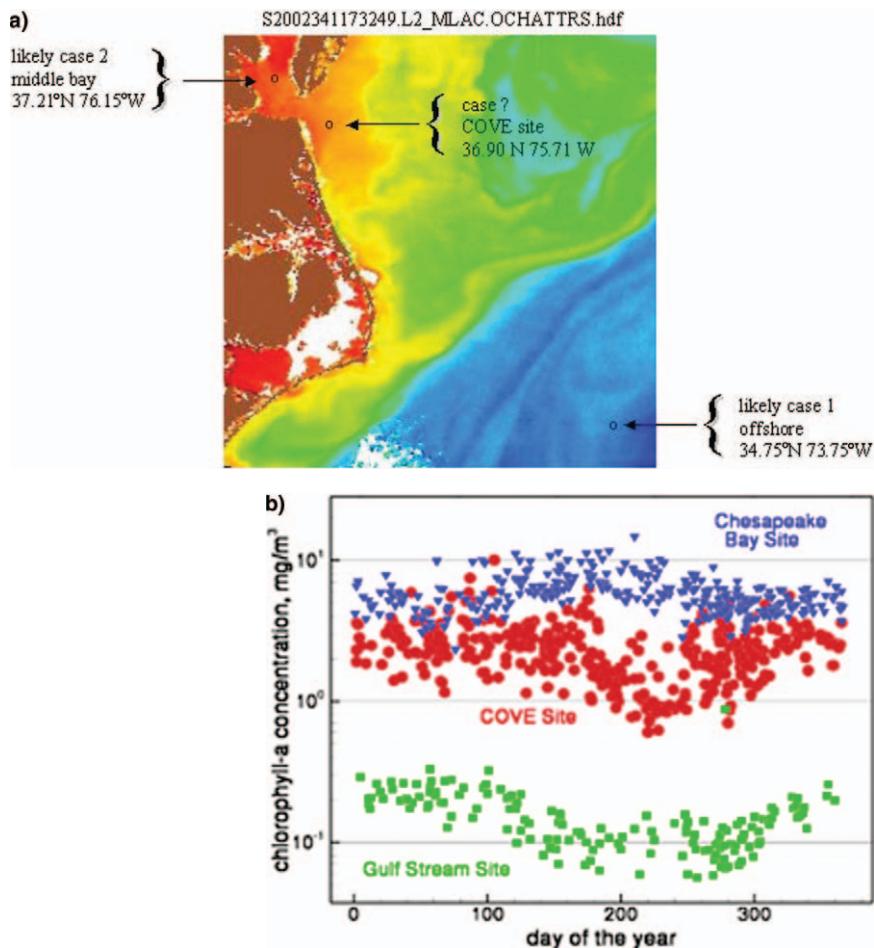
Ocean color radiances. Old Dominion University's Center for Coastal and Physical Oceanography performs spectral water–leaving radiance observa-tions continuously, and in-water optics observations with water samples for wet-laboratory analyses intermittently, since midyear 2001. These measurements are used to test coastal zone retrieval algorithms for NASA's Moderate Resolution Imaging Spectroradiometer (MODIS) ocean color program. In support of ocean color research for MODIS and the Sea-Viewing Wide Field-of-View Sensor (SEAWIFS), NASA's AERONET program recently deployed an ocean-scanning photometer (SeaPRISM—SeaWiFS Photometer Revision for Incident Surface Measurement). This instrument scans both the sky and ocean to retrieve the visible spectral water–leaving radiances. These observations have been used for testing ocean color satellite retrievals. The ocean color radiance instruments are located on the tower top at the COVE site [Fig. 2(G)].

OCEAN–ATMOSPHERE REGIONAL CHARACTERIZATION.

We have implemented COVE at a location over the ocean to benefit from the dark and spatially homogeneous surface properties of ocean. When the surface is dark and homogeneous, the effect of surface albedo on scattered radiation is reduced, and this key input to a radiative transfer model can be specified with more confidence. This reduces the "wiggle room" of uncertainty for model inputs and allows calculated irradiances to be compared with observations at a tougher standard. But, are the properties of the ocean and atmosphere at COVE similar to those of the open ocean? Some answers follow.

Ocean color. A freshwater plume that often exits at the mouth of the Chesapeake Bay affects many factors associated with the inner continental shelf areas of the Mid-Atlantic Bight [physical: Boicourt (1981), Roman and Boicourt (1999); biological: Rutledge and Marshall (1981), Grothues and Cowen (1999); chemical: Bates and Hansell (1999)]. We have used satellite-derived ocean color data to address this issue. The ocean color community classifies natural waters into two categories. In "case 1" (usually open ocean) waters, the water-leaving radiances are primarily altered by chlorophyll-a and other components that naturally covary with it (other chlorophylls, zooplankton, and degradation products). In "case 2" (often coastal) waters, chlorophyll, colored dissolved organic matter, and sediment loads combine to modulate the water-leaving radiances in a more complex way (Sathyendranath 2000).

Clear-sky chlorophyll-a retrievals from the SeaWiFS instrument were used to compare the ocean color of

a) S2002341173249.L2_MLAC.OCHATTRS.hdf

likely case 2
middle bay
37.21°N 76.15°W

case ?
COVE site
36.90 N 75.71 W

likely case 1
offshore
34.75°N 73.75°W

b)

Chesapeake
Bay Site

COVE Site

Gulf Stream Site

Fig. 3. (a) Typical clear-sky chlorophyll-a retrieval (false color) from the SeaWiFS instrument aboard the SeaStar spacecraft for a region that is in the vicinity of COVE. To assess the optical classification of waters at the COVE site, an arbitrary site beyond the Gulf Stream waters off the North Carolina coast and a site in the middle of the lower Chesapeake Bay were chosen for representing case-1 and case-2 waters (respectively). (b) Summary of six years of clear-sky retrievals of chlorophyll-a concentrations (mg m^{-3}) retrieved by the SeaWiFS sensor for three sites. For most of the year, the COVE site chlorophyll-a is comparable to the bay site (case 2), but distinct chlorophyll concentration groups emerge during summer months. These ocean color data suggest that the water surrounding the COVE site should be classified as having the case-2 water type.

the water at the COVE site relative to nearby locations shown in Fig. 3a. By assuming the water classification for the offshore Atlantic Ocean location to be case 1 and the classification for the water in the middle of the Chesapeake Bay to be case 2, we can characterize the COVE site relative to these locations.

The results of six years of SeaWiFS retrievals (Fig. 3b) suggest that the COVE site's chlorophyll concentrations and hence ocean color is more similar to the bay site than the open-ocean site. The bay plume appears to have an influence on the ocean color at COVE for all periods of the year. These results demonstrate that the ocean color at COVE is hardly ever similar to the open-ocean site (case 1). But the map (Fig. 3a) has false color. Using the online Coupled Ocean Atmosphere Radiative Transfer (COART) model (Jin et al. 2005) and assuming chlorophyll concentrations of 0.2 mg m^{-3} for case 1, 2 mg m^{-3} for COVE, and 5 mg m^{-3} for case 2, we calculate broadband surface albedos (solar zenith angle of 20° and wind speed of 5 m s^{-1}) of 0.032 for case 1, 0.034 for COVE, and 0.036 for case 2. All three locations have low broadband albedos.

Aerosol characteristics. Urban and continental aerosol size distributions are typically dominated by fine-mode particles (having radii less than about 0.6 μm), while desert and maritime aerosols are typically dominated by coarse-mode particles (radii greater than 0.6 μm). Although the Chesapeake Lighthouse is located 25 km from the nearest landmass, the aerosols at this location are generally dominated by small particle sizes; they are consistent with urban/continental aerosols (Fig. 4).

Predominantly westerly winds cause aerosols from the North American continent to pass over COVE regularly. Our back-trajectory analysis (not shown) for the 1999–2003 time period using NOAA's Hybrid Single-Particle Lagrangian Integrated Trajectory (HYSPLIT) model (see information online at www.arl.noaa.gov/ready/hysplit4.html) indicates that 67% of the 1-day trajectories originate over the northeast United States and another 23% of the trajectories originate over the southern United States.

Wintertime aerosol optical depths (AODs) at COVE typically correspond to clean conditions, with monthly averages of about 0.08 at 0.5 μm dur-
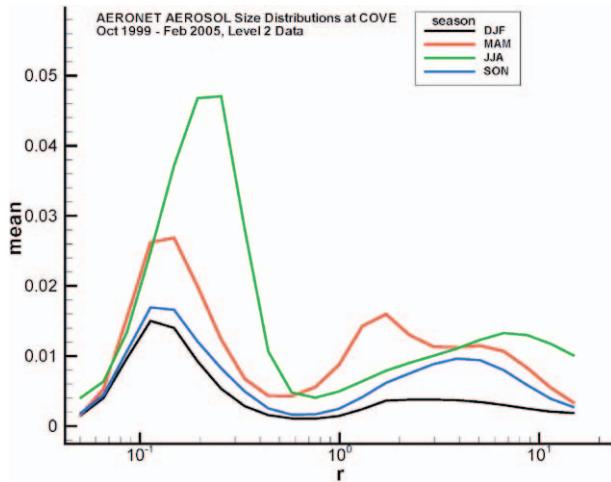
Fig. 4. Seasonal averages of aerosol volume distributions derived from AERONET observations made at the COVE site; x-axis (r) radius of aerosol particles (μm), y-axis mean volume of aerosol particles (dV/dlnr). Averages were taken from 41 months of level-2 data (from October 1999 to February 2005, inclusive). The fine-mode variation is correlated with changes in the precipitable water (PW) within the atmospheric column; summer (JJA) has the highest precipitable water concentration, winter (DJF) has the lowest precipitable water concentration.

ing December through February (not shown). The AOD increases throughout the spring until it peaks at monthly averaged values of about 0.35 during the hazy summers months (June through August). The summertime peak in AOD occurs during the same time of year that the total column precipitable water vapor peaks, indicating that hygroscopic particles play a significant role in solar attenuation for the summertime aerosols.

The seasonal variability of the atmospheric aerosols at COVE is also exhibited in the aerosol size distributions at the site. Figure 4 shows the seasonal-averaged aerosol size distributions at the COVE site (downloaded from the AERONET database). All of the distributions are multimodal, with a relative minimum at a radius of about 0.6 μm. The solid black line of Fig. 4 corresponds to the relatively pristine conditions of the winter months [December–February (DJF)], with low concentrations of both the fine and coarse modes. The spring months of the

March–May show an increase in both modes. The hazy summer months [June–August (JJA)] have the most pronounced fine mode. These results indicate that the aerosols over the COVE site are not typical of marine environments (which are characterized by greater volumes for the coarse modes).

Cloud climatology. The cloud conditions at any specific surface observation site play an important part in altering the downwelling shortwave and longwave irradiances. We used an algorithm developed by Long and Ackerman (2000) that is based on radiation measured at the site to infer the percentage of sky (e.g., 0%–3% = clear, 97%–100% = overcast) that is obscured by clouds. Figure 5 shows the monthly mean percent clear, overcast, and partly cloudiness for the September 2000–January 2004 time period. The annual trend for clear skies show the summer months to have the fewest periods of clear skies (June–August: approximately 10%), while the month of October has the highest occurrence of clear skies (35%). May has the highest occurrence of overcast skies, and the summer months (JJA) have the highest occurrence of partly cloudy skies (approximately 60%).

SCIENCE PROBLEMS FOR COVE. The site is presently well equipped for ocean–atmosphere radiation studies in clear skies. We are implementing instruments for in situ aerosol properties in 2006 to augment the existing retrievals and to provide aerosol
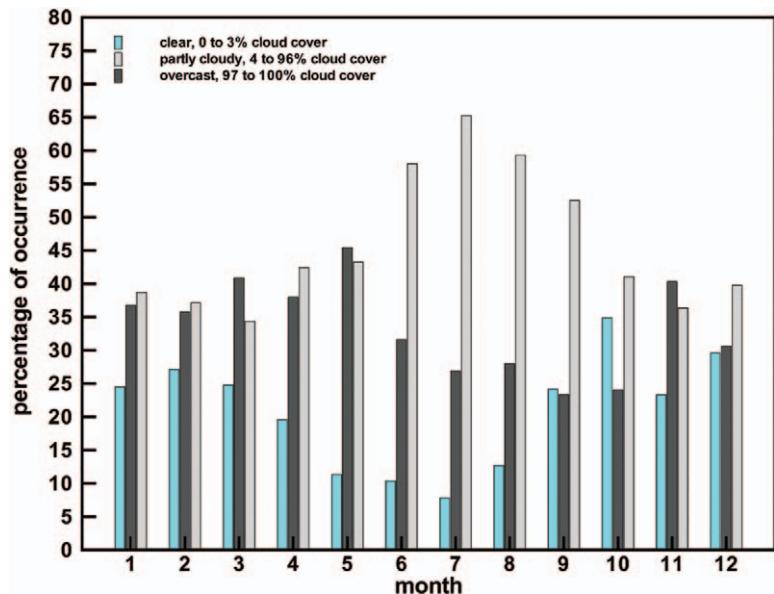
Fig. 5. Monthly cloud coverage (based on Long and Ackerman 2000) derived from radiation observations made at the COVE site. Clear, partly cloudy, and overcast conditions are based upon 15-min radiation observations. Daytime only.

information under cloudy skies. The aerosol in situ instrumentation suite includes the following:

- a condensation nuclei counter that counts all particles with diameters greater than 0.010 μm,
- a cloud condensation nuclei counter that counts all aerosol particles capable of activating into cloud drops at supersaturations common to clouds,
- an aethelometer for measuring the aerosol absorption coefficient at seven wavelengths,
- wet and dry nephelometers for measuring wet and dry aerosol scattering at one wavelength (the combination of wet and dry scattering measurements also provide an indication of the aerosol hygroscopic growth), and
- an electrical aerosol detector that provides the average diameter of accumulation mode aerosols (i.e., aerosols with diameters from 0.01 to 1 μm).

An optimal future for projects at COVE would include instrumentation to observe cloud microphysical properties and quantities. This would allow the COVE radiometry system to be applied to a wide range of complexity that the atmosphere can produce from clouds and aerosols.

Some of the clear-sky issues we have addressed to date are discussed below.

CERES irradiance retrieval at the surface. How does the retrieval of surface irradiance for the ocean surface scene type at COVE compare to other scene types found on the planet? To answer this question, we can compare retrieved CERES surface irradiances to observations at COVE and also to observations from other surface observation sites from various scene types (snow, desert, cropland, grassland, shrubland, etc.). This comparison is made possible by using the CERES ARM Validation Experiment (CAVE; Rutan et al. 2001), a Web-accessible archive of time-synchronized surface observations and CERES products (available online at www-cave.larc.nasa/gov/cave/). We have used the *Terra* edition 2B Surface and Atmosphere Radiation Budget (SARB) products from CAVE for this clear-sky-only comparison (Charlock et al. 2005).
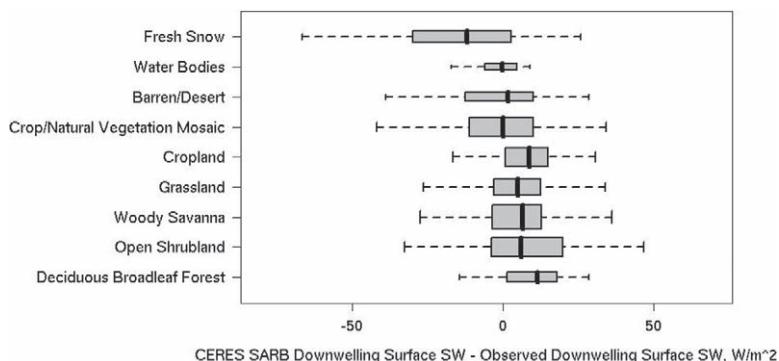
Fig. 6. Box-and-whiskers plots indicating distributions of differences between surface observations and CERES SARB estimates of downwelling shortwave global radiation at the surface for nine surface scene types under clear skies. Data were included if 1) the cloud imager and the Long and Ackerman (2000) cloud index reported 0% clouds, 2) the percentage of the scene type was greater than 50% in the CERES instrument field of view, and 3) the sun-glint angle was between 30° and 80°. For retrieving the surface irradiances, CERES uses a modified version (Rose and Charlock 2002) of the Fu and Liou (1993) radiative transfer model. Inputs to the radiative transfer model include aerosols and cloud properties from MODIS aboard *Terra,* gridded fields of temperature, humidity, wind (*GEOS-4*; Bloom et al. 2005), and ozone from National Centers for Environmental Prediction (NCEP) Stratospheric Monitoring Group Ozone Blended Analysis.

For each surface type, the difference distribution between the retrieved and observed surface irradiance is shown (Fig. 6). The medians (center bands) of the distributions for the water bodies group and crop/natural vegetation mosaic group indicate the smallest differences between retrieved versus observed (their medians fall close to the "0"). The largest differences are found in the fresh snow group and the deciduous broadleaf forest group (median falls farthest from "0"). The water bodies group has the smallest dispersion and the fresh snow group has the largest.

The largest contrast between surface types is found when comparing the fresh snow and the water bodies groups. The retrieval over snow (which has the highest broadband albedo) is poor. Its median is farthest from the zero and its dispersion is the largest of all the groups. The retrievals over water bodies (which have the lowest albedo) show near-zero bias and the smallest dispersion. Ninety percent of the water bodies group is made up of observations from the COVE site. The existing oceanic island sites offer precious few clear-sky observations that synchronize with the CERES SARB.

The low surface albedo over water surfaces permits a more accurate MODIS retrieval of AOD, which is a key input for the flux calculation. The fresh snow scene type with its high albedo results in the largest dispersion and bias of all the scene types. The snow

albedo is often inhomogeneous too. If the large albedo near an observation site differs from that over the mean of the large CERES field of view, multiple scattering will cause a bias in the CERES calculation. Retrieving the necessary parameters for input into the models is more difficult over the snow scene type. Here, the ocean's low albedo appears to make the retrieved insolation more accurate. The other scene types fall in between these two groups with respect to retrieval performance.

Ocean albedo parameterization. The COVE broadband and spectral irradiance data have been used for validation purposes in a parameterization of ocean albedo (not shown here) using the COART model (Jin et al. 2004). This radiative transfer model accounts for a layered atmosphere and a layered ocean as a continuum of characteristic optical properties, after accounting for the change in refractive index at the surface. The parameterization was developed to allow global climate models access to a dynamic ocean albedo based on multiyear observations of albedo as a function several parameters (optical depth, solar cosine zenith, wind speed, and concentrations of chlorophyll-a). The ocean albedo parameterization results may be obtained at the following Web site: http://snowdog.larc.nasa.gov/jin/getocnlut.html. These results are being used operationally by CERES to determine ocean albedo for input to the radiative transfer calculations.

SUMMARY. NASA's CERES project is performing high-quality ocean environment shortwave and longwave radiation observations required for climate change research on a unique radiation-monitoring site located on an ocean platform. Observation methods of the BSRN are used to provide the most accurate ocean environment long-term radiation measurements available. The collocation of several observation networks at the site provides valuable information for verifying algorithms associated with radiation transfer mechanisms involving the ocean and atmosphere.

The waters surrounding the COVE site are indicative of the case-2 waters, but the broadband albedo calculated for the site is not much different from case-1 (open ocean) waters. The aerosols are characteristic of continental/urban aerosols, not marine aerosols. Agreement between comparisons of CERES-retrieved surface shortwave irradiance to the observed shortwave parameters obtained at the COVE site show negligible bias and have the smallest variability when compared to other scene types representing the planet's surface. Ocean albedo studies have been summarized and are now available for use in global climate models.

The anticipated value of establishing a radiation-monitoring site to benefit from the low surface reflective properties of the ocean is being realized at COVE. The accumulation of long-term radiation observations from COVE should prove valuable for future testing of retrieval algorithms required for satellite-based instruments.

APPENDIX: GLOSSARY OF TERMS.

Radiant energy

Radiance	Radiant energy confined to a solid angle or cone. The angular measure to define the cones uses steradians. Radiance units are energy per area per time per frequency and per steradian (e.g., W m^{-2} nm sr^{-1}, recall W = J s^{-1}). The collection cone is oriented in space so radiance observations are always associated with a direction.
Irradiance	Radiant energy incident upon a surface. Irradiance units are energy per time and per area (e.g., W m^{-2}). Atmospheric sensors view an entire hemisphere [2 π (pi) sr].

Spectral regions

Shortwave	Wavelengths containing energy emitted by the sun (sometimes called solar wavelengths). This spectral region spans wavelengths from 0.2 to 5.0 μm.

Longwave	Wavelengths containing energy emitted at terrestrial temperatures (sometimes called infrared thermal wavelengths). This spectral region spans wavelengths from 5 to 50 μm.
Broadband	Radiation measurements over the entire shortwave or longwave spectral regions.
Narrowband	Radiation measurements over a discrete spectral range of wavelengths, for example, from 0.50 to 0.55 μm.
PAR	Photosynthetically active radiation; the spectral region from 0.4 to 0.7 μm; this range includes wavelengths efficiently absorbed by various types of chlorophylls found in plants and phytoplankton.

Field of view

Global	Irradiance measurement, hemispheric field of view, includes direct and diffuse components.
Direct	Irradiance measurement of solar beam typically limited to 5° field of view.
Diffuse	Irradiance measurement with an instrument shaded from the direct solar beam (hemispheric field of view).

Instruments

Pyranometer	Irradiance measurement of shortwave energy.
Pyrgeometer	Irradiance measurement of longwave energy.
Pyrheliometer	Irradiance measurement of direct component of the solar energy.
Pyrometer	Radiance measurement of longwave energy.
MFRSR	Multifilter Rotating Shadowband Radiometer; shaded and unshaded narrowband irradiance measurements.
Sunphotometer	Direct narrowband radiance measurements at multiple wavelengths.

REFERENCES

Bates, N. R., and D. A. Hansell, 1999: A high resolution study of surface layer hydrographic and biogeochemical properties between Chesapeake Bay and Bermuda. *Mar. Chem.,* **67,** 1–16.

Bloom, S., and Coauthors, 2005: Documentation and validation of the Goddard Earth Observing System (GEOS) data assimilation system—Version 4. Tech. Rep. Series on Global Modeling and Data Assimilation 104606, Vol. 26, 161 pp. [Available online at http://gmao.gsfc.nasa.gov/systems/geos4/.]

Boicourt, W. C., 1981: Circulation in the Chesapeake Bay entrance: Estuary-shelf interactions. *Proc. of the Chesapeake Bay Plume Study, Superflux 1980,* Williamsburg, VA, NOAA and NASA, NASA Conf. Publication 2188, 61–78.

Bruegge, C. J., J. E. Conel, R. O. Green, R. O. Margolis, R. G. Holm, and G. Toon, 1992: Water vapor column abundance retrievals during FIFE. *J. Geophys. Res.,* **97,** 18 759–18 768.

Businger, S., and Coauthors, 1996: The promise of GPS in atmospheric monitoring. *Bull. Amer. Meteor. Soc.,* **77,** 5–18.

Castanho, A. D. A., J. Vanderlei Martins, P. Artaxo, L. Remer, and M. Yamasoe, 2005: Chemical characterization of aerosols on the East Coast of the United States using aircraft and ground based stations during the CLAMS Experiment. *J. Atmos. Sci.,* **62,** 934–946.

Charlock, T. P., F. G. Rose, D. A. Rutan, L. H. Coleman, T. Caldwell, and S. Zentz, 2005: Global multiyear analysis of CERES Terra observations and radiative transfer calculations. *Proc. 15th ARM Science Team Meeting,* Daytona Beach, FL, ARM. [Available online at www.arm.gov/publications/proceedings/conf15/extended_abs/charlock_tp.pdf.]

Chowdhary, J., and Coauthors, 2005: Retrieval of aerosol scattering and absorption properties from photopolarimetric observations over the ocean during the CLAMS experiment. *J. Atmos. Sci.,* **62,** 1093–1117.

Duan, J., and Coauthors, 1996: GPS meteorology: Direct estimation of the absolute value of precipitable water. *J. Appl. Meteor.,* **35,** 830–838.

Dubovik, O., and M. D. King, 2000: A flexible inversion algorithm for retrieval of aerosol optical properties from Sun and sky radiance measurements. *J. Geophys. Res.,* **105,** 20 673–20 696.

——, A. Smirhov, B. N. Holben, M. D. King, Y. J. Kaufman, T. F. Eck, and I. Slutsker, 2000: Accuracy assessments of aerosol optical properties retrieved from AERONET sun and sky-radiance measurements. *J. Geophys. Res.,* **105,** 9791–9806.

Fu, Q., and K.-N. Liou, 1993: Parameterization of the radiative properties of cirrus clouds. *J. Atmos. Sci.,* **50,** 2008–2025.

Gatabe, C. K., M. D. King, A. I. Lyaspustin, G. T. Arnold, and J. Redemann, 2005: Airborne spectral measurements of ocean directional reflectance. *J. Atmos. Sci.,* **62,** 1072–1092.

Grothues, T. M., and R. K. Cowen, 1999: Larval fish assemblages and water mass history in a major faunal transition zone. *Contin. Shelf Res.,* **19,** 1171–1198.

Holben, B. N., and Coauthors, 1998: AERONET—A federated instrument network and data archive for aerosol characterization. *Remote Sens. Environ.,* **66,** 1–16.

——, and Coauthors, 2001: An emerging ground-based aerosol climatology: Aerosol optical depth from AERONET. *J. Geophys. Res.,* **106** (D11), 12 067–12 097.

Ignatov, A., and Coauthors, 2005: Two MODIS aerosol products over ocean on the *Terra* and *Aqua* CERES SSF datasets. *J. Atmos. Sci.,* **62,** 1008–1031.

Jin, Z., T. P. Charlock, W. L. Smith Jr., and K. Rutledge, 2004: A parameterization of ocean surface albedo. *Geophys. Res. Lett.,* **31,** L22301, doi:1001029/2004GL021180.

——, and Coauthors, 2005: Radiation measurement and model simulation for the CLAMS experiment. *J. Atmos. Sci.,* **62,** 1053–1071.

Kahn, R., and Coauthors, 2005: MISR calibration and implications for low-light-level aerosol retrieval over dark water. *J. Atmos. Sci.,* **62,** 1032–1051.

Levy, R. C., L. A. Remer, J. V. Martins, Y. J. Kaufman, A. Plana-Fattori, J. Redemann, and B. Wenny, 2005: Evaluation of the MODIS aerosol retrievals over ocean and land during CLAMS. *J. Atmos. Sci.,* **62,** 947–973.

Long, C. N., and T. P. Ackerman, 2000: Identification of clear skies from broadband pyranometer measurements and calculation of downwelling shortwave cloud effects. *J. Geophys. Res.,* **105,** 15 609–15 626.

Magi, B. I., P. V. Hobbs, T. W. Kirchstetter, T. Novakov, D. A. Hegg, S. Gao, J. Redemann, and B. Schmid, 2005: Aerosol properties and chemical apportionment of aerosol optical depth at locations off the United States East Coast in July and August 2000. *J. Atmos. Sci.,* **62,** 919–933.

McArthur, L. J. B., 2005: Baseline Surface Radiation Network (BSRN). WCRP/WMO Operations Manual, WMO/TD 1274, 176 pp.

Ohmura, A., and Coauthors, 1998: Baseline Surface Radiation Network (BSRN/WRMC), a new precision radiometry for climate research. *Bull. Amer. Meteor. Soc.,* **79,** 2115–2136.

Payne, R. E., 1972: Albedo of the sea surface. *J. Atmos. Sci.,* **29,** 959–970.

Redemann, J., and Coauthors, 2005: Suborbital measurements of spectral aerosol optical depth and its variability at sub-satellite-grid scales in support of CLAMS. *J. Atmos. Sci.,* **62,** 993–1007.

Remer, L. A., and Coauthors, 2005: The MODIS aerosol algorithm, products, and validation. *J. Atmos. Sci.,* **62,** 947–973.

Roman, M. R., and W. C. Boicourt, 1999: Dispersion and recruitment of crab larvae in the Chesapeake Bay plume: Physical and biological controls. *Estuaries,* **22,** 563–574.

Rose, F. G. and Charlock, T. P., 2002: New Fu-Liou code tested with ARM raman lidar aerosols and CERES in pre-CALIPSO sensitivity study. Preprints, *11th Conf. on Atmospheric Radiation,* Ogden, UT, Amer. Meteor. Soc., CD-ROM, P4.8.

Rutan, D. A., F. G. Rose, N. Smith, and T. P. Charlock, 2001: Validation data set for CERES Surface and Atmospheric Radiation Budget (SARB). *GEWEX News,* Vol. 11, No. 1 (February), 11–12. [Available online at www.gewex.com under "Newsletter".]

Rutledge, C. K., and H. G. Marshall, 1981: Use of ordination and classification procedures to evaluate photoplankton communities during Superflux II. *Proc. Chesapeake Bay Plume Study, Superflux 1980,* Williamsburg, VA, NOAA and NASA, NASA Conf. Publication 2188, 469–490.

Sathyendranath, S., Ed., 2000: Remote sensing of ocean colour in coastal, and other optically-complex, waters. IOCCG Rep. No. 3, 144 pp.

Smirnov, A., B. N. Holben, T. F. Eck, O. Dubovik, and I. Slutsker, 2000: Cloud screening and quality control algorithms for the AERONET database. *Remote Sens. Environ.,* **73,** 337–349.

Smith, W. L., Jr., T. P. Charlock, R. Kahn, J. V. Martins, L. A. Remer, P. V. Hobbs, J. Redemann, and C. K. Rutledge, 2005: EOS *Terra* aerosol and radiative flux validation: An overview of the Chesapeake Lighthouse and Aircraft Measurements for Satellites (CLAMS) experiment. *J. Atmos. Sci.,* **62,** 903–918.

Smith, W. L., Sr., D. K. Zhou, A. M. Larar, S. A. Mango, H. B. Howell, R. O. Knuteson, H. E. Revercomb, and W. L. Smith Jr., 2005: The NPOESS airborne sounding testbed interferometer remotely sensed surface and atmospheric conditions during CLAMS. *J. Atmos. Sci.,* **62,** 1118–1134.

Welton, E. J., J. R. Campbell, J. D. Spinhirne, and V. S. Scott, 2001: Global monitoring of clouds and aerosols using a network of micro-pulse lidar systems. *Lidar Remote Sensing for Industry and Environmental Monitoring,* U. N. Singh, T. Itabe, and N. Sugimoto, Eds., *Proc. SPIE,* **4153,** 151–158.

Wielicki, B. A., B. R. Barkstrom, E. F. Harrison, B. B. Lee III, G. L. Smith, and J. E. Cooper, 1996: Clouds and the Earth's Radiant Energy System (CERES): An earth observing system experiment. *Bull. Amer. Meteor. Soc.,* **77,** 853–868.